A Method of Multi-component Signal Detection Based on Differential Nonlinear Mode Decomposition

Tiantian Yang, Jie Shao, Yue Huang, and Reza Malekian

***Abstract*—In order to detect the multi-component signal from the noise and chaos, a method based on the differential nonlinear mode decomposition (DNMD) is proposed in this paper. This new analysis approach applies the differential to the original signal. Then the nonlinear mode decomposition (NMD) is used to obtain a series of meaningful nonlinear modes, which has the advantage of extracting high frequency components with small amplitudes and learns from the superiority of NMD such as noise robust. Finally, spectrum analysis is used to the decomposed components. The analysis of simulation signals and the real underwater signal is given to demonstrate the effectiveness of this method. The proposed method can detect multi-component signals of time-varying amplitude without fake frequency under the condition of noise and chaos. Compared with traditional decomposition methods, the peaks of Hilbert marginal spectrum of proposed method are sharper, and $\overline{R_2}, \overline{R_3}$ are higher.**

***Index Terms*—Multi-component signal detection, Differential nonlinear mode decomposition, Chaos, Spectrum analysis**

I. INTRODUCTION

ADAPTIVE time-frequency analysis methods have wide range of applications, such as speech signals analysis [1], sonar signals processing [2] and mechanical fault diagnosis [3]. There are numerous observable chaotic signals in the natural phenomena, such as ambient acoustic noise in ocean and clutter induced by an electromagnetic pulse directed at the ocean surface [4].

Manuscript received March 26, 2018; revised June 23, 2018. Date of publication June 29, 2018. Prof. Nikola Rožić has been coordinating the review of this manuscript and approved it for publication.

Tiantian Yang, Jie Shao and Yue Huang are with the Key Laboratory of Radar Imaging and Microwave Photonics (Nanjing Univ. Aeronaut. Astronaut.), Ministry of Education, College of Electronic and Information Engineering, Nanjing University of Aeronautics and Astronautics, Nanjing, 210016, China (e-mails: yeungtt1992@163.com, shaojie@nuaa.edu.cn, huangyuexl@163.com).

Reza Malekian is with the Department of Electrical, Electronic and Computer Engineering, University of Pretoria, Pretoria, 0002, South Africa (e-mail: reza.malekian@ieee.org).

This work was supported in part by the Open Project Program of the Key Laboratory of Underwater Acoustic Signal Processing (Southeast University), China's Ministry of Education (No. UASP1604), the Fundamental Research Funds for the Central Universities (No. 2242016K3001), A Project Funded by the Priority Academic Program Development of Jiangsu Higher Education Institutions, National Research Foundation, South Africa (grant numbers: IFR160118156967 and RDYR160404161474).

Digital Object Identifier (DOI): 10.24138/jcomss.v14i2.514

In the past, FFT is used to analyze signals because of its simplicity and efficient computation, but there are three major pitfalls, namely aliasing, picket-fence effect and leakage [5]. FFT is not suitable for detecting the time-varying signals. Chirp-Z transform is one of the spectrum zooming methods to estimate frequency [6]. Discrete chirp-Fourier transform (DCFT) can be used to analyze multicomponent chirp signals [7]. A procedure based on the radial-basis-function (RBF) neural network is proposed to detect the amplitudes of the multi component signals [8]. However, RBF neural network has an inevitable training process. The training is typically done in two phases, first fixing the width and centers and then the weights. More numerical operations are used in the RBF to increase the accuracy. A method based on convex optimization is proposed in [9], but weak signals are not easy to be recognized because some shape peaks exist in the detection result figures.

The methods of decomposition of non-linear signal are studied in recent years. Empirical mode decomposition (EMD) [10,11] separates complicated signals into a series of intrinsic mode functions (IMFs), then Hilbert spectrum is used to represent the time-frequency distribution. In addition, the marginal spectrum is offered a measure of total amplitude (or energy) contribution from each frequency value. EMD is widely used in non-linear and non-stationary data analysis [12]. When the amplitudes of signals are less than the boundary of the hard slope, the EMD does not separates the signals [13]. The major drawback of EMD is the mode mixing, that is to say, one IMF includes wide disparate scales or a similar scale appears in different IMFs. In order to solve this problem, the ensemble empirical mode decomposition (EEMD) [14] adds white Gaussian noise of finite amplitude to the signals and utilizes EMD. The above two methods have a disadvantage that they are quite sensitive to noise.

Nonlinear mode decomposition (NMD) [15] decomposes a signal into a number of physically meaningful oscillations. Compared with the previous methods, NMD is a new adaptive decomposition tool with the advantage of noise-robust [16]. Differential nonlinear mode decomposition (DNMD) is put forward in this paper, which synthesizes the strengths of current methods. Numerical simulation results have shown that the proposed method has better performance on extracting small amplitude signals under noise and chaos. The method based on DNMD shows advantages over other methods in quantitative comparisons. In the case of underwater acoustic

signal, proposed method can remove effectively the ocean ambient noise and detect both signals when the amplitude of one signal is smaller than another signal.

II. BACKGROUND

Nonlinear mode decomposition is a new adaptive decomposition tool proposed in 2015[15]. NMD is based on the time-frequency analysis techniques, surrogate data tests, and the identification of the time-variable harmonics. NMD extracts all physically meaningful modes, removes noise and has excellent performance at noise robustness. The NMD result can be expressed as

$$s(t)=\sum_i c_i(t)+n(t) \tag{1}$$

where $s(t), c_i(t)$ and $n(t)$ are the original signal, the i th Nonlinear Mode(NM) and the noise, respectively. The main algorithm of NMD is described as follows.

(1) Calculate the original signal's wavelet transform (WT) $W_s(\omega,t)$,

$$W_s(\omega,t)=\int_{-\infty}^{\infty} s^+(u)\psi^*\left[\frac{\omega(u-t)}{\omega_\psi}\right]\frac{\omega du}{\omega_\psi} \tag{2}$$
$$=\frac{1}{2\pi}\int_0^{\infty} e^{i\xi t}\hat{s}(\xi)\hat{\psi}^*\left(\frac{\omega_\psi \xi}{\omega}\right)d\xi$$

$$s^+(t)=\int_{0^+}^{\infty}\hat{s}(\xi)e^{i\xi t}d\xi \tag{3}$$

$$\hat{\psi}(\xi)=e^{-(2\pi f_0\ln\xi)^2/2} \tag{4}$$

where $f_0=1$, $\hat{s}(\xi)$ is the Fourier transform of $s(t)$, $\psi(t)$ denotes a log-normal wavelet and $\hat{\psi}(\xi)$ is the Fourier transform of $\psi(t)$. $\omega_\psi=\arg\max|\hat{\psi}(\xi)|$ denotes wavelet peak frequency.

(2) Find all h th ridge curves $\omega_p^{(h)}(t)$ of WT, ridge curve can be defined as the sequence of WT amplitude peaks into which most of the energy of that component is mapped at each time. At time t, h points of the position of peaks $\omega_p(t)=\underset{\omega\in[\omega_-(t),\omega_+(t)]}{\arg\max}|W_s(\omega,t)|$. All the $\omega_p(t)$ form the h ridge curve [17].

(3) Obtain the amplitude $A^{(h)}(t)$, phase $\phi^{(h)}(t)$, and frequency $v^{(h)}(t)$ from $\omega_p^{(h)}(t)$

$$\text{WT:}\begin{cases} v^{(h)}(t)=\omega_p^{(h)}(t)e^{\delta\ln v_d^{(h)}(t)} \\ A^{(h)}(t)e^{i\phi^{(h)}(t)}=\dfrac{2W_s(\omega_p^{(h)}(t),t)}{\hat{\psi}^*[\omega_\psi v^{(h)}(t)/\omega_p^{(h)}(t)]} \end{cases} \tag{5}$$

$$v^{(h)}(t)\equiv\phi'^{(h)}(t) \tag{6}$$

(4) Check whether WT is the optimal TFR type, if not, switch windowed Fourier transform (WFT) $G_s(\omega,t)$

$$G_s(\omega,t)\equiv\int_{-\infty}^{\infty} s^+(u)g(u-t)e^{-i\omega(u-t)}dt \tag{7}$$
$$=\frac{1}{2\pi}\int_0^{\infty} e^{i\xi t}\hat{s}(\xi)\hat{g}(\omega-\xi)d\xi$$

where $g(t)$ is a Gaussian window for the WFT , $\hat{g}(\xi)$ meets the condition: $\hat{g}(0)=\max|\hat{g}(\xi)|$.

$$\hat{g}(\xi)=e^{-(f_0\xi)^2/2}\Leftrightarrow g(t)=\frac{1}{\sqrt{2\pi}f_0}e^{-(t/f_0)^2/2} \tag{8}$$

Then re-extract the ridge curves and harmonics,

$$\omega_p(t)=\underset{\omega\in[\omega_-(t),\omega_+(t)]}{\arg\max}|G_s(\omega,t)| \tag{9}$$

$$\text{WFT:}\begin{cases} v^{(h)}(t)=\omega_p^{(h)}(t)+\delta v_d^{(h)}(t) \\ A^{(h)}(t)e^{i\varphi^{(h)}(t)}=\dfrac{2G_s(\omega_p^{(h)}(t),t)}{\hat{g}[\omega_p^{(h)}(t)-v^{(h)}(t)]} \end{cases} \tag{10}$$

$$v^{(h)}(t)\equiv\phi'^{(h)}(t) \tag{11}$$

where $\delta\ln v_d^{(h)}(t)$ and $\delta v_d^{(h)}(t)$ are the correction for discretization effects found by parabolic interpolation.

(5) Compute the possible h th harmonic $x^{(h)}(t)=A^{(h)}(t)\cos\phi^{(h)}(t)$.

(6) Calculate the significance level,

$$\text{significance level}=\frac{N_{D_s>D_0}}{N_s} \tag{12}$$

$$D(\alpha_A,\alpha_v)=\alpha_A Q\left[\hat{A}(\xi)\right]+\alpha_v Q\left[\hat{v}(\xi)\right] \tag{13}$$

$$Q[f(x)]\equiv-\int\frac{|f(x)|^2}{\int|f(x)|^2dx}ln\frac{|f(x)|^2}{\int|f(x)|^2dx}dx \tag{14}$$

where $N_{D_s>D_0}$ is the number of surrogates with $D_s>D_0$ and N_s is the number of surrogates. D is the degree of order in the amplitude $A(t)$ and frequency $v(t)$, Q is spectral entropy of $A(t)$ and $v(t)$. D_0 corresponds to the h th harmonic, $D_{s=1\cdots N_s}$ corresponds to surrogates. In order to confirm the value of D, this paper calculates $D(1,0), D(0,1)$ and $D(1,1)$, and then selects the maximum among them.

(7) Compute amplitude-phase consistency $\rho^{(h)}$

$$\rho^{(h)}(w_A,w_\phi,w_v)=(q_A^{(h)})^{w_A}(q_\phi^{(h)})^{w_\phi}(q_v^{(h)})^{w_v} \tag{15}$$

$$\begin{cases} q_A^{(h)} \equiv \exp\left\{-\dfrac{\sqrt{\left\langle\left[A^{(h)}(t)\left\langle A^{(1)}(t)\right\rangle - A^{(1)}(t)\left\langle A^{(h)}(t)\right\rangle\right]^2\right\rangle}}{\left\langle A^{(1)}(t)A^{(h)}(t)\right\rangle}\right\}, \\ q_\phi^{(h)} \equiv a\left|\left\langle \exp\left\{i\left[\phi^{(h)}(t) - h\phi^{(1)}(t)\right]\right\}\right\rangle\right|, \\ q_\nu^{(h)} \equiv \exp\left\{-\dfrac{\sqrt{\left\langle\left[\nu^{(h)}(t) - h\nu^{(1)}(t)\right]^2\right\rangle}}{\left\langle \nu^{(h)}(t)\right\rangle}\right\} \end{cases} . \quad (16)$$

where w_A, w_ϕ, w_ν are the weights of $q_A^{(h)}, q_\phi^{(h)}, q_\nu^{(h)}$.

(8) When both amplitude-phase consistency $\rho^{(h)} \geq 0.25$ and the significance level is ≥ 0.95, harmonic is identified as true.

(9) Constitute one NM $c_i(t)$ using the first harmonic and true higher harmonics.

(10) Subtract the NM from the signal and repeat (1)-(9). If the first harmonic does not pass the surrogate test against noise, and therefore NMD is stopped.

III. Multi-component Signal Detection Based on DNMD

In the actual situation, the low power signals are inevitably masked by noise. To solve the problem of extracting multi component time-varying signal, a new detecting method based on the differential nonlinear mode decomposition is proposed. Differential operation can enlarge the power of small part and make it easier to be detected. In order to analyze the signal deeply, spectrum analysis is applied after decomposition. The effect of suppressing noise and chaos is improved by twice decomposition. The algorithm of this novel method is carried out in the following steps.

Step 1: Apply differential to the original signal $s(t)$ to get the new signal $s'(t)$;

Step 2: Apply NMD to $s'(t)$ to get NMs $c_i'(t)$;

Step 3: Integrate $c_i'(t)$ to get $b_i(t)$;

Step 4: Apply NMD to each $b_i(t)$, we only extract the first NM of the $b_i(t)$ and regard it as the $c_i(t)$ of the original signal. Each NM contains fundamental and harmonics while each IMF contains only one mode of oscillation. The residue of the signal is removed in DNMD.

Step 5: Complete Hilbert marginal spectrums to $c_i(t)$. Hilbert spectrum is defined as follows

$$H(\omega,t) = \mathrm{Re}\left[\sum_{i=1}^{n} a_i(t)\exp\left(j\int \omega_i(t)dt\right)\right] \quad (17)$$

where $a_i(t)$ and $\omega_i(t)$ are the instantaneous amplitude and instantaneous frequency of $z_i(t) = c_i(t) + j\hat{c}_i(t)$. $\hat{c}_i(t)$ represents Hilbert transform of $c_i(t)$. So the Hilbert marginal spectrum is

$$h(\omega) = \int_0^T H(\omega,t)dt \quad (18)$$

To quantitatively compare these methods, the ratio R_i [18] is calculated in this paper by

$$R_i = \frac{A_i}{E} \quad (19)$$

where subscript i means ith component, A_i represents the peak of ith component and E denotes mean value of the spectrums of the decomposed component. The higher R_i is, the better performance of the detection method is. $\overline{R}_i$ is the mean value of R_i.

IV. Numerical Simulation and Analysis

After describing the DNMD procedure, this paper illustrates the effectiveness of the proposed method by considering the following simulation signals [19, 20]. All the tests are carried out using MATLAB R2012b on a desktop Intel Core i7-455U PC with Windows 8 system. The sampling frequency of the signal is 400Hz. A Monte Carlo simulation of 100 replications is conducted for this section. In our paper, *SNR* is the ratio of the signal power to the noise power, and it does not include chaos.

A. Example 1

A multi-component signal of time-varying amplitude under white noise is described as follows,

$$\begin{aligned} yp(t) &= \sum_{i=1}^{3} s_i(t) \\ s_1(t) &= A_1(t)\cos(2\pi f_1 t + 0.5\sin(2\pi t/2)) \\ s_2(t) &= A_2(t)\cos(2\pi f_2 t + \sin(2\pi t/2)) \\ s_3(t) &= A_3(t)\cos(2\pi f_3 t + 6\sin(2\pi t/2)) \\ A_1(t) &= a_1(1 + 0.25\cos(2\pi f_1 t/20)), \\ A_2(t) &= a_2(1 + 0.15\cos(2\pi f_2 t/20)), \\ A_3(t) &= a_3(1 + 0.2\cos(2\pi f_3 t/20)), \end{aligned} \quad (20)$$

$$y_1(t) = yp(t) + n(t) \quad (21)$$

where $f_1 = 10\text{Hz}$, $f_2 = 45\text{Hz}$, $f_3 = 100\text{Hz}$, $a_1 = 1$, $a_2 = 0.5$, $a_3 = 0.3$ and $n(t)$ is a white noise. The time domain waveform of signal $y_1(t)$ under $SNR = 10\text{dB}$ is depicted in Fig. 1.

For the convenience of comparisons, the Hilbert marginal spectrums of decomposition of signal $y_1(t)$ are presented in Fig. 2. DNMD and NMD can clearly extract each component signal and the peak of each component is sharper because of good noise robustness (see Fig. 2a and Fig. 2b). There are no obvious peaks near the 45Hz and the spectrums are flat at 100Hz because noise interference is serious in Fig. 2c and Fig. 2d, so EMD and EEMD fail to obtain small component signals and these methods only detect the components of $s_1(t)$ and

$s_2(t)$. There is a fake frequency about 5Hz at the beginning of the EMD spectrum (as shown in Fig. 2c).

In order to compare the performance of DNMD quantitatively, the ratio $\overline{R}_i$ of each method under different SNR is listed in Table I. According to the Table I, superiority of $\overline{R}_1$ in DNMD is not obvious. $\overline{R}_2$ and $\overline{R}_3$ of DNMD are higher than that of NMD. When SNR decreases to 10dB, DNMD and NMD can both detect the $s_3(t)$, $\overline{R}_2$ of DNMD is 5.1191 higher than that of NMD. The results of EMD and EEMD still do not meet expectations. Therefore, DNMD performs better than the other decomposition methods.

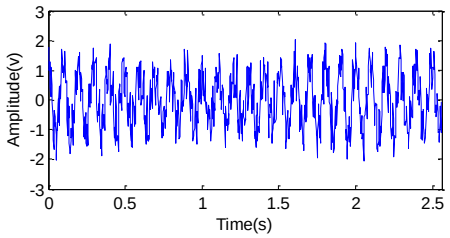

Fig. 1. The time domain waveform of signal $y_1(t)$.

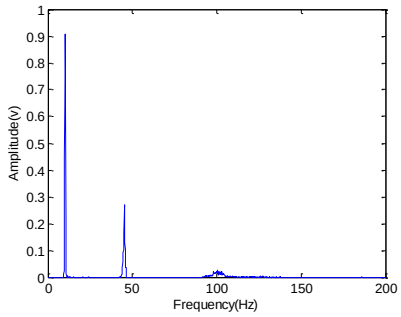

(a) DNMD

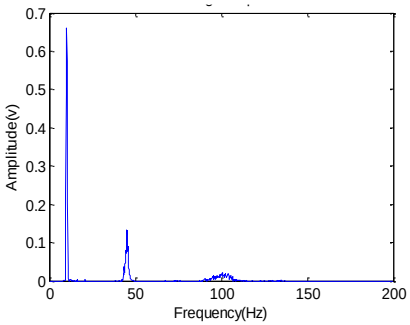

(b) NMD

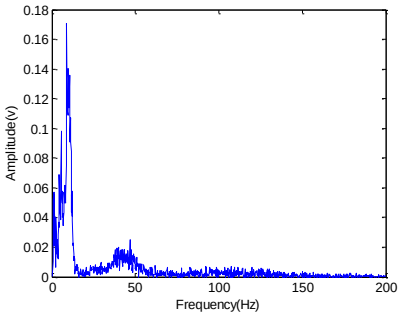

(c) EMD

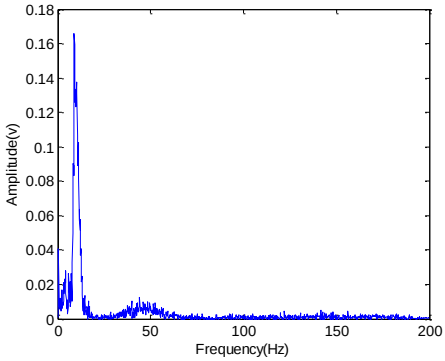

(d) EEMD

Fig. 2. Hilbert marginal spectrum of signal $y_1(t)$

TABLE I
THE RATIO $\overline{R}_i$ OF EACH METHOD UNDER DIFFERENT SNR

SNR /dB		DNMD	NMD	EMD	EEMD
20	$\overline{R}_1$	196.0085	184.4007	113.6896	86.6355
	$\overline{R}_2$	54.5923	43.7354	11.4991	13.9559
	$\overline{R}_3$	6.6695	6.5119	NA	NA
15	$\overline{R}_1$	164.2211	174.0197	44.8732	45.5927
	$\overline{R}_2$	50.5447	36.4610	6.0942	8.2387
	$\overline{R}_3$	5.5624	5.3189	NA	NA
10	$\overline{R}_1$	145.2083	165.2165	28.1738	30.1645
	$\overline{R}_2$	37.8538	32.7347	3.8026	4.4622
	$\overline{R}_3$	5.2101	4.6806	NA	NA
5	$\overline{R}_1$	135.5067	187.9332	23.8997	32.0115
	$\overline{R}_2$	16.8437	24.0974	NA	NA
	$\overline{R}_3$	NA	NA	NA	NA

B. *Example 2*

Chaotic signals are commonly existed in the natural phenomena. A chaotic signal looks like a random noise, which is generated by a determinate system. When the signal is polluted by white noise and chaotic signals, DNMD can also extract the original signal. The chaotic interference signal is generated by Lorenz system which is a simplified mathematical model for atmospheric convection at first.

Lorenz system, as a typical chaos, is commonly added to signal analysis. The equation can be described as follows:

$$\begin{cases} \dot{x} = \sigma(y - x) \\ \dot{y} = -xz + rx - y \\ \dot{z} = xy - bz \end{cases} \tag{22}$$

Where $\sigma = 10,\ r = 28,\ b = 8/3,$ the initial value is $x_0 = y_0 = z_0 = 0.1$ [9].

Here take its x component. To further validate effectiveness

of DNMD, another simulated signal $y_2(t)$ is discussed. $a_1 = 1,\ a_2 = 0.3,\ a_3 = 0.08$ and $d_1(t) = 0.02x$ is the chaotic signal.

$$y_2(t) = yp(t) + n(t) + d_1(t) \tag{23}$$

When SNR=15dB, the time domain wave of signal $y_2(t)$ is presented in Fig 3. The Hilbert marginal spectrums of each method are shown in Fig. 4. The ratios $\overline{R}_i$ of each method under different *SNR* are listed in Table II. In the Table II, SIR is the ratio of signal power to interference (noise and chaos) power.

As shown in Fig. 4, when decreasing the amplitude of $s_2(t)$ and $s_3(t)$, DNMD still detects all the component signals. NMD loses the third component. The spectral peaks of $s_2(t)$ in DNMD and NMD are sharper than that of EMD and EEMD.

As listed in Table II, when *SNR* decreases to 10dB, DNMD also detects the third component signal unsuccessfully. However, $\overline{R}_2$ in DNMD are larger than that of NMD. When $SNR = 5\text{dB}$, $\overline{R}_2 = 13.2948$ in DNMD and $\overline{R}_2 = 12.9949$ in NMD. DNMD can suppress the noise and chaos effectively and reflect more information from the signal. It is demonstrated in Table II that DNMD is superior to other methods under the same condition of noise and chaos.

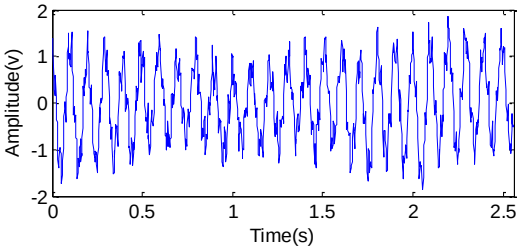

Fig. 3. The time domain wave of signal $y_2(t)$

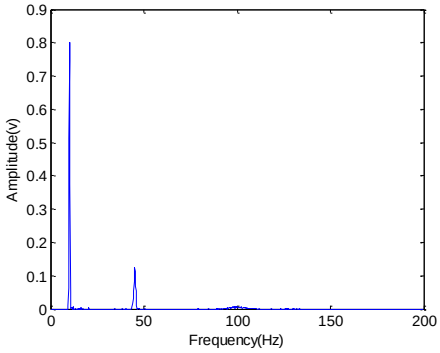

(a) DNMD

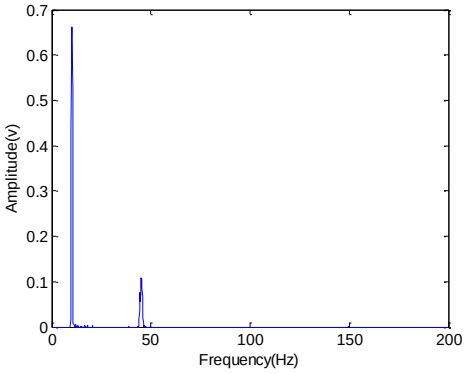

(b) NMD

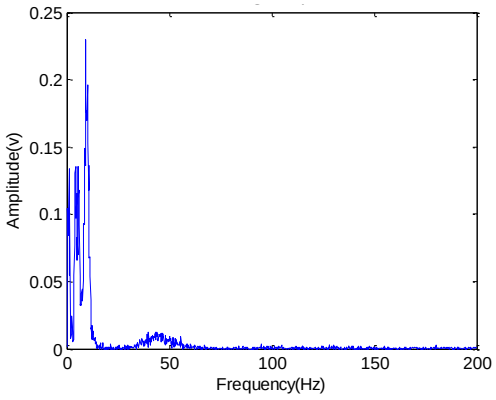

(c) EMD

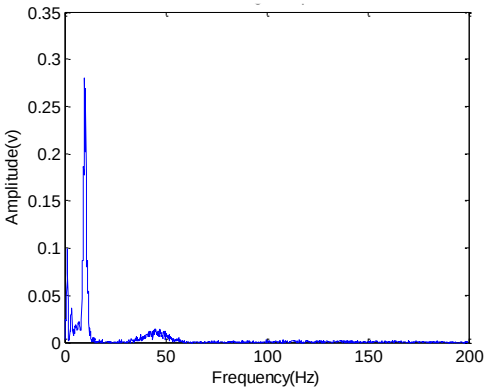

(d) EEMD

Fig. 4. Hilbert marginal spectrum of signal $y_2(t)$

The time cost of each method is listed in Table III. The running time of DNMD is longer because of the higher algorithmic complexity and better performance of detection, which matches our anticipation. As we all know, time consumption and performance of the method can't be achieved at the same time.

TABLE II
THE RATIO $\overline{R_i}$ OF EACH METHOD UNDER DIFFERENT SNR

SNR /dB	SIR /dB		DNMD	NMD	EMD	EEMD
20	12.89	$\overline{R_1}$	215.3318	232.6214	67.5781	104.6944
		$\overline{R_2}$	48.1808	33.7599	3.4137	5.7904
		$\overline{R_3}$	2.0685	NA	NA	NA
15	11.28	$\overline{R_1}$	206.1982	203.7725	43.1689	56.8438
		$\overline{R_2}$	26.5790	19.6764	2.3779	3.4724
		$\overline{R_3}$	1.9004	NA	NA	NA
10	8.16	$\overline{R_1}$	220.9171	238.3432	39.4086	35.9182
		$\overline{R_2}$	23.9773	20.0645	NA	NA
		$\overline{R_3}$	NA	NA	NA	NA
5	4.32	$\overline{R_1}$	172.8786	205.9586	30.0629	37.5047
		$\overline{R_2}$	13.2948	12.9949	NA	NA
		$\overline{R_3}$	NA	NA	NA	NA

TABLE III
THE TIME COST OF EACH METHOD

	DNMD	NMD	EMD	EEMD
running time/s	244.919	113.050	0.474	11.415

V. REAL SIGNAL ANALYSIS

Ocean ambient noise is colored noise and an interference signal. Industrial activities, ship noise, wind and rain are main noise source off the coast. In this section, DNMD is used to detect the real underwater signal. The vertical underwater acoustic array data was collected in shallow-water off the Italian west coast by the NATO SACLANT Center in La Spezia, Italy. The sample frequency is 1kHz. The frequency of the signal is about 170Hz and 350Hz. The data used here was collected by the third sensor. Actually, the frequency are near 170Hz and 330Hz after analysis. A multi component signal analyzed here consists of this two single frequency signals.

$$y_3(t) = sf_1(t) + \beta \cdot sf_2(t) \tag{24}$$

where $sf_1(t)$ denotes the signal of 170Hz, $sf_2(t)$ denotes the signal of 330Hz and β is a coefficient used to adjust the amplitude of $sf_2(t)$.

When $\beta = 1$, the time waveform and FFT of $y_3(t)$ are depicted in Fig. 5 and Fig. 6. There is a certain degree of apophysis near 100Hz in Fig. 6, which means ocean ambient noise is relatively strong. The Hilbert marginal spectrums of the signal decomposed by each method are shown in Fig. 7. According to Fig. 7, all methods can detect the 170Hz and 330Hz to some extent. However, the spectrum of DNMD and NMD are cleaner than traditional decomposition method. DNMD and NMD remove more noise and interference. The performance of eliminating the effect of the ocean ambient noise in EMD, EEMD is weak.

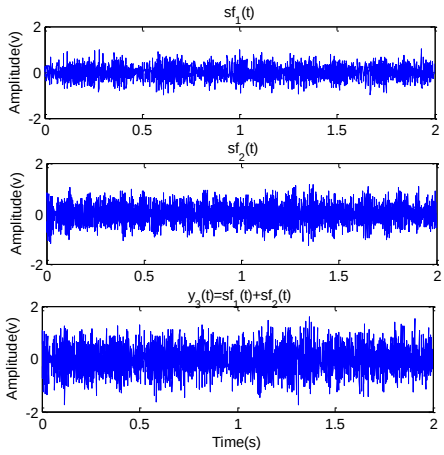

Fig. 5. The time domain wave of underwater acoustic signal

$$y_3(t) = sf_1(t) + sf_2(t)$$

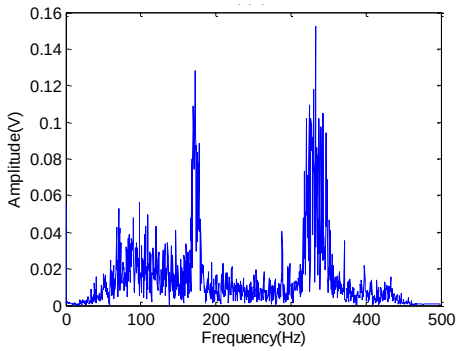

Fig. 6. The FFT spectrum of underwater acoustic signal

$$y_3(t) = sf_1(t) + sf_2(t)$$

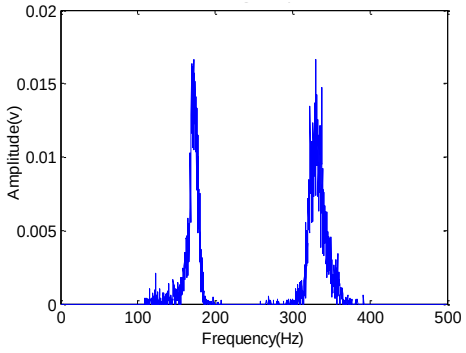

(a) DNMD

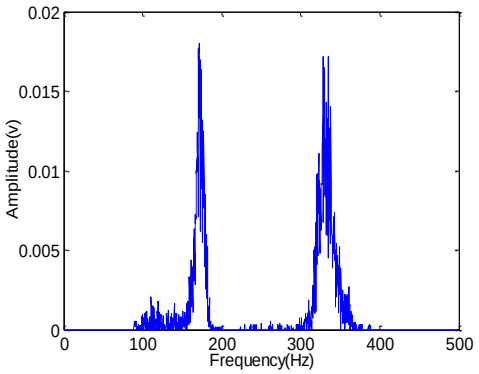

(b) NMD

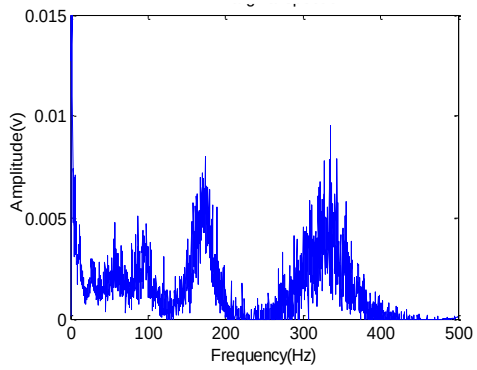

(c) EMD

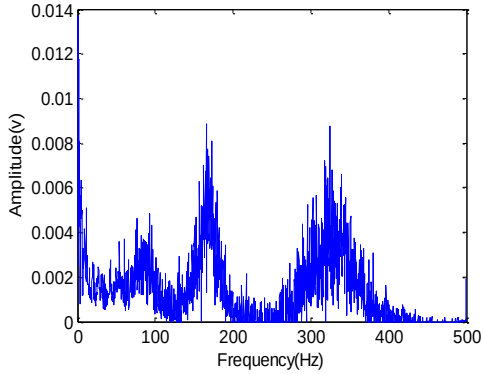

(d) EEMD

Fig. 7 Hilbert marginal spectrum of underwater acoustic signal

$$y_3(t) = sf_1(t) + sf_2(t)$$

When $\beta = 0.23$, DNMD is more effective than other methods. The time waveform and the FFT spectrum of signal $y_3(t) = sf_1(t) + 0.23sf_2(t)$ are shown in Fig. 8 and Fig. 9, respectively. The Hilbert marginal spectrums of this condition are shown in Fig. 10. There are two peaks near 290Hz and 370Hz in Fig. 9, which is easy to be recognized as useful frequencies. From Fig. 10a and Fig.10b, DNMD suppresses ocean ambient noise and detects the 170Hz and 330Hz while NMD only extracts the 170Hz. It's difficult to find single frequency in Fig. 10c and Fig.10d because EMD and EEMD suffer from noise seriously.

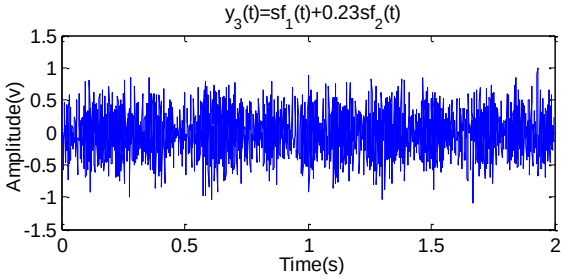

Fig 8. The time domain wave of underwater acoustic signal

$$y_3(t) = sf_1(t) + 0.23sf_2(t)$$

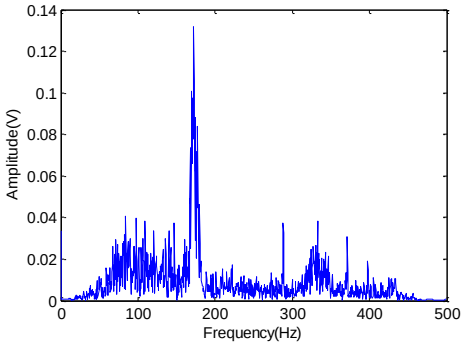

Fig. 9. The FFT spectrum of underwater acoustic signal

$$y_3(t) = sf_1(t) + 0.23sf_2(t)$$

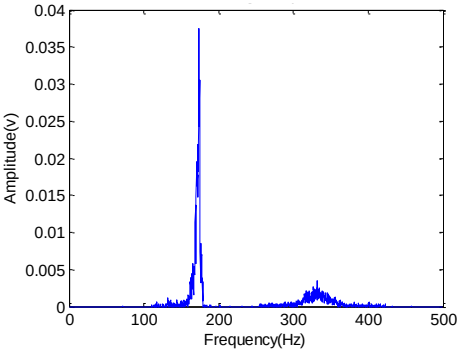

(a) DNMD

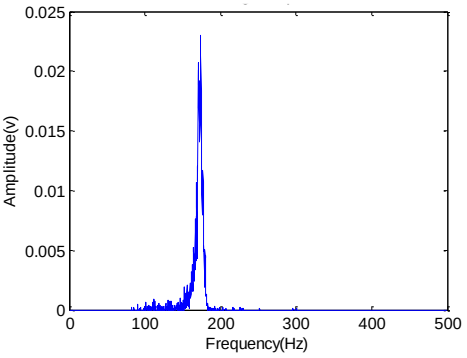

(b) NMD

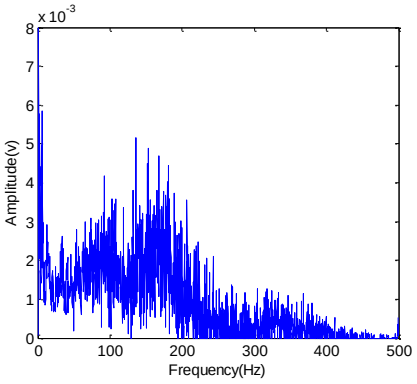

(c) EMD

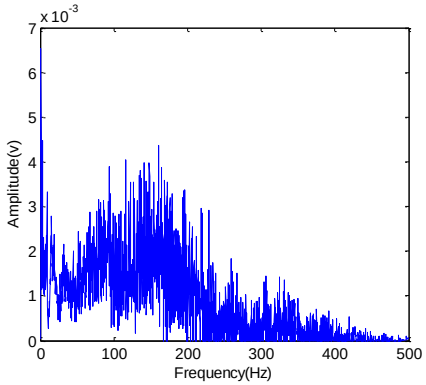

(d) EEMD

Fig. 10. Hilbert marginal spectrum of underwater acoustic signal

$$y_3(t) = sf_1(t) + 0.23sf_2(t)$$

VI. CONCLUSION

In this paper, a new method based on DNMD is proposed to analyze the non-linear and non-stationary signal and to detect multi-component time-varying signal. Firstly, the differential is applied to the original signal. The NMD is utilized to obtain a series of physically meaningful oscillations. Then, spectrum analysis is used to the decomposed components. The proposed method solves the problem of extracting relatively high frequency components with small amplitudes and is less sensitive to noise and chaos comparing with EMD and EEMD.

From the simulation signals, the proposed method can detect the more component signals under white Gaussian noise and chaotic interference. There is no fake frequency in the DNMD Hilbert spectrum. This approach holds on to the favorable position when changing the amplitude of signal. $\overline{R_2}, \overline{R_3}$ of DNMD are almost larger than that of NMD. From the real data analysis, our method still maintains the superiority under the condition of ocean ambient noise.

According to discussion and comparisons, it has demonstrated that DNMD is an efficient and appropriate approach to signal decomposition. DNMD can be used to obtain each component from the multicomponent signal under noise, chaos and ocean ambient noise.

REFERENCES

[1] C. Tantibundhit, F. Pernkopf and G. Kubin, "Joint Time–Frequency Segmentation Algorithm for Transient Speech Decomposition and Speech Enhancement,"*IEEE Transactions on Audio Speech & Language Processing*, vol.18, no.6, pp. 1417-1428, Aug. 2010. DOI: 10.1109/TASL.2009.2035037.

[2] G. C. Gaunaurd and H. C. Strifors, "Signal analysis by means of time-frequency (Wigner-type) distributions-applications to sonar and radar echoes," *Proceedings of the IEEE*, vol.84, no.9, pp. 1231-1248, Sep. 1996. DOI: 10.1109/5.535243.

[3] D. Yu, J. Cheng and Y. Yang, "Application of EMD method and Hilbert spectrum to the fault diagnosis of roller bearings," *Mechanical Systems & Signal Processing*, vol.19, no.2, pp. 259-270, Mar. 2005. DOI: 10.1016/S0888-3270(03)00099-2.

[4] G. Manjunath, S. S. Ganesh and G. V. Anand, "Denoising signals corrupted by chaotic noise," *Communications in Nonlinear Science & Numerical Simulation*, vol.15, no.12, pp. 3988-3997, Dec. 2010. DOI: 10.1016/j.cnsns.2010.01.015.

[5] A. A. Girgis and F. M. Ham, "A Quantitative Study of Pitfalls in the FFT," *IEEE Transactions on Aerospace & Electronic Systems*, vol.16, no.4, pp. 434-439. Jul. 1980. DOI: 10.1109/TAES.1980.308971.

[6] WX. Zhang, XJ. Liu, XW. Chen, et al. "A NSZT Method for Frequency Estimation and Anti-noise Performance Analysis," *Chinese Journal of Electronics*, vol. 27, no. 3, pp. 648-657. May. 2018. DOI: 10.1049/cje.2017.10.007.

[7] J. Li, B. Li, Z. Guo, et al. "Multicomponent Chirp Signal Detection Based on Discrete Chirp-Fourier Transform," *Wireless Personal Communications*, vol.96, no.4, pp. 1-13. Oct. 2017. DOI: 10.1007/s11277-017-4392-z.

[8] G. W. Chang, C. I. Chen and Y. F. Teng, "Radial-Basis-Function-Based Neural Network for Harmonic Detection," *IEEE Transactions on Industrial Electronics*, vol.57, no.6, pp. 2171-2179, Jun. 2010. DOI: 10.1109/TIE.2009.2034681.

[9] J. Hu, Y. Zhang, Yang M, et al. "Weak harmonic signal detection method from strong chaotic interference based on convex optimization," *Nonlinear Dynamics*, vol.84, no.3, pp. 1469-1477, Jan. 2016. DOI: 10.1007/s11071-015-2582-3.

[10] N. E. Huang, Z. Shen, Long S R, et al. "The empirical mode decomposition and the Hilbert spectrum for nonlinear and non-stationary time series analysis," *Proceedings of the Royal Society of London, Series*, vol.454, no. 12, pp.903-995, Mar. 1998. DOI: http://www.jstor.org/stable/53161.

[11] B. Weng and K. E. Barner, "Optimal Signal Reconstruction Using the Empirical Mode Decomposition," *Eurasip Journal on Advances in Signal Processing*, vol.2008, no.1, pp. 1-12, Dec. 2008. DOI: 10.1155/2008/845294.

[12] W. Tong, M. Zhang, Q. Yu, et al. "Comparing the applications of EMD and EEMD on time–frequency analysis of seismic signal," *Journal of Applied Geophysics*, vol.83, pp. 29-34, Aug. 2012. DOI: 10.1016/j.jappgeo.2012.05.002.

[13] M. Feldman, "Analytical basics of the EMD: Two harmonics decomposition," *Mechanical Systems & Signal Processing*, vol.23, no.7, pp. 2059-2071. Oct. 2009. DOI: 10.1016/j.ymssp.2009.04.002

[14] Z. Wu and N. E Huang. "Ensemble empirical mode decomposition: a noise-assisted data analysis method," *Advances in Adaptive Data Analysis*, vol.1, no.1, pp. 1-41, Jan. 2009. DOI: 10.1142/S1793536909000047.

[15] D. Iatsenko, P. V. Mcclintock and A. Stefanovska, "Nonlinear mode decomposition: a noise-robust, adaptive decomposition method," *Physical Review E Statistical Nonlinear & Soft Matter Physics*, vol.92, no.3, pp. 1-25, Sep. 2015. DOI: 10.1103/PhysRevE.92.032916

[16] Z. Xin, S. Jie, Wenwei A, et al. "An Improved Time-Frequency Representation based on Nonlinear Mode Decomposition and Adaptive Optimal Kernel," Elektronika ir Elektrotechnika, vol.22, no.4, pp. 52-57, Mar. 2016. DOI: 10.5755/j01.eie.22.4.15918.

[17] D. Iatsenko, P. V. E. McClintock and A .Stefanovska, "Linear and synchrosqueezed time–frequency representations revisited: Overview, standards of use, resolution, reconstruction, concentration, and algorithms," *Digital Signal Processing*, vol.42, pp. 1-26, Apr. 2015. DOI: 10.1016/j.dsp.2015.03.004.

[18] D. Wang, Q. Miao, Fan X, et al. "Rolling element bearing fault detection using an improved combination of Hilbert and wavelet transforms," *Journal of Mechanical Science & Technology*, vol.23, no.12, pp. 3292-3301. Dec. 2009. DOI: 10.1007/s12206-009-0807-4.

[19] Jingcun Yu, Reza Malekian, Jianghao Chang, Benyu Su, "Modeling of Whole-Space Transient Electromagnetic Responses Based on FDTD and its Application in the Mining Industry", IEEE Transactions on Industrial Informatics, Vol. 13, no.6, pp. 2974 - 2982, 2017. DOI: 10.1109/TII.2017.2752230.

[20] Ning Ye, Zhong-qin Wang, Reza Malekian, Qiaomin Lin, and Ru-chuan Wang, "A Method for Driving Route Predictions Based on Hidden Markov Model", Mathematical Problems in Engineering, Vol.2015, pp.1-12, 2015. DOI:10.1155/2015/824532

Tiantian Yang received the B.S. degree in electronic Science and Technology in 2015 from the Nanjing University of Posts and Telecommunications, Nanjing, China. Since September 2015, She has been studying for her MS degree in circuit and system in Nanjing University of Aeronautics and Astronautics, Nanjing, China. Her research interests include signal detection and processing.

Jie Shao is currently an Associate Professor with the College of Electronics and Information Engineering, Nanjing University of Aeronautics and Astronautics, China. His major research interests include signal detection and intelligent information processing.

Yue Huang was born in Anhui, China, received the BS degree in electronic information engineering in 2014 from the Hefei University, Hefei, China. Since September 2015, he has been studying for his MS degree in electronics and communication engineering in Nanjing University of Aeronautics and Astronautics, Nanjing, China. His current research interests include electronic system design and signal processing.

Reza Malekian (M'12-SM'17) is an Associate Professor and Head of Advanced Sensor Network Research Group with the Department of Electrical, Electronic, and Computer Engineering, University of Pretoria, Pretoria, South Africa. His research interests include advanced sensor networks, Internet of Things, and mobile communications. Dr. Malekian is the Joint-Chapter Chair of IEEE Signal Processing and Communications Societies, South Africa section and a chapters committee member of the IEEE Signal Processing representative of region 8. He is also a Chartered Engineer and a Professional Member of the British Computer Society and an associate editor for *IEEE Internet of Things Journal* and *IEEE Transactions on Intelligent Transportation Systems*.